Revista Brasileira de Cartografia (2014) N^0 66/7 - International Issue: 1413-1436
Sociedade Brasileira de Cartografia, Geodésia, Fotogrametria e Sensoriamento Remoto
ISSN: 1808-0936

REMOTE SENSING OF AMAZONIAN FORESTS: MONITORING STRUCTURE, PHENOLOGY AND RESPONSES TO ENVIRONMENTAL CHANGES

Sensoriamento Remoto da Floresta Amazônica: Monitoramento da Estrutura, Fenologia e das Respostas às Mudanças Ambientais

João Roberto dos Santos, Lênio Soares Galvão &
Luiz Eduardo Oliveira e Cruz de Aragão

Instituto Nacional de Pesquisas Espaciais – INPE
Divisão de Sensoriamento Remoto – DSR/OBT
Av. dos Astronautas, 1758, 12.227-010 – São José dos Campos - Brasil
{jroberto, lenio, laragao}@dsr.inpe.br

Recebido em 18 de Outubro, 2013/ Aceito em 8 de Dezembro, 2013
Received on October 18, 2013/ Accepted on December 8, 2013

ABSTRACT

Remote sensing is a key tool for studying the tropical Amazonian forests, which have a substantial role on the global climate system and on the carbon and water cycles. In this article, we overview recent advances in remote sensing for estimating tropical forest structure and biomass, for analyzing phenological patterns across tropical landscapes, and for quantifying the impacts of natural and human-induced environmental changes on this ecosystem. This review highlighted the importance of the combined use of optical and microwave data and of the integration of the remote sensing products with the field-based information for understanding the functioning of Amazonian ecosystems, its composition and the stressing factors (e.g., deforestation, fire, droughts) that can directly impact this biome.

Keywords: Impacts of Environmental Changes, Forest inventory, Biomass Modeling, Phenological Forest Patterns, Forest Degradation.

RESUMO

Sensoriamento remoto é uma ferramenta essencial para estudar florestas tropicais Amazônicas, que têm um papel fundamental no clima global e nos ciclos de carbono e água. Neste artigo revisamos recentes avanços em sensoriamento remoto para estimar biomassa e estrutura de florestas tropicais, para analisar padrões fenológicos regionais, e para quantificar os impactos das mudanças ambientais naturais e induzidas pelo homem sobre este ecossistema. Esta revisão destacou a importância do uso combinado de dados ópticos e de micro-ondas e da integração dos produtos de sensoriamento remoto com informação de campo para compreender o funcionamento do ecossistema Amazônico, sua composição e os fatores de estresse (p.ex., desflorestamento, queimadas, secas) que podem diretamente afetar este bioma.

Palavras-chave: Impactos das Mudanças Ambientais, Inventário Florestal, Modelagem de Biomassa, Padrões da Fenologia Florestal, Degradação Florestal.

1. INTRODUCTION

Amazonia is the world's largest continuous tropical forest playing a substantial role on the global climate system (HOUGHTON *et al*. 2000). This biome covers an area of about 5.3 million km^2 of humid lowland undisturbed rainforest (EVA; HUBER 2005), accounting for 40% of the global tropical forest area. Because of its dimension, any perturbations within this system can have significant global impacts on the climate and on the carbon and water cycles. Even small, changes in the functioning of this ecosystem are likely to produce significant climatic feedbacks (COX *et al*. 2004).

Three major processes operate in opposite directions determining the role of Amazonia on the climate system: (1) the natural absorption of carbon from the atmosphere, through the photosynthesis process, and its subsequent fixation in the biomass, resulting in forest growth (MALHI *et al.* 1998); (2) the reduction in forest ecosystem productivity because of the impact of increased temperature and/or severity of droughts on net primary productivity, ecosystem respiration and mortality rates (CLARK 2004, PHILLIPS *et al*. 2009), which reduces the magnitude of the natural C sink; and (3) the human-induced emissions of greenhouse gases into the atmosphere, as a result of land use practices such as deforestation and biomass burning. The balance between these processes will determine the role of Amazonia in mitigating or accelerating climate impacts.

For instance, Amazonian undisturbed forests are estimated to be a major tropical C sink in the global C budget (PAN *et al*., 2011), which contributed to a sustained sink of 0.47 (0.34 – 0.59) Pg C yr^{-1} since the 1980's (PHILLIPS *et al*., 2009). Conversely, DeFries *et al.* (2002) and Aguiar *et al.* (2012) estimate that deforestation in Amazonia was a net C source of 0.28 (0.17–0.49) Pg C yr^{-1} during the 1990s and 0.10-0.15 Pg C yr^{-1} for 2009, respectively. Quantification of these processes over massive geographical areas is critical for countries to evaluate the status of their natural resources. It is estimated that gross deforestation in this region, which converted a total of ~ 765,000 Km^2 of primary forest into other land uses to date (http://www.obt.inpe.br/prodes/), is responsible for 75% of Brazilian greenhouse gases emissions, around 20% of global emissions of (MCT, 2010). Maintaining the stability of these stocks is, hence, critical for countries such as Brazil, which hosts approximately 75% of the total Amazonian area, to contribute to climate change mitigation.

In the context of Amazonia, which implies in a large geographical area with dynamic processes operating at multiple scales, remote sensing is a key tool that allows the quantification of carbon stocks in forest biomass, the evaluation of seasonal changes in forest canopy, which ultimately will determine the direction and magnitude of carbon, water and energy flows between the canopy and the atmosphere, and the monitoring of stressing factors that controls the changes in forest biomass through time. The importance of remote sensing on these issues is reflected in the increased number of publications since the 1980s (Figure 1).

In this article, we aim to provide an overview of the recent developments of remote sensing technology that allowed the scientific community to advance in these three fronts cited above. We will examine the contribution of: (1) RADAR remote sensing for estimating tropical forest structure and biomass; (2) multi-temporal optical remote sensing for analyzing phenological patterns across tropical landscapes;

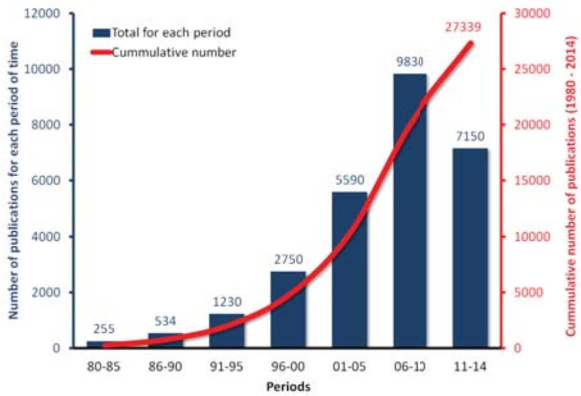

Fig. 1 - Trend in the number of papers published focusing on remote sensing of Amazonian forests. The results presented are based on Google Scholar searching tool using "Remote Sensing" + Amazon as keywords. The figure demonstrates that, since early 1980s, the number of articles published annually on the theme increased from 255 (1980-1985) to 7150 (2014), totalizing by the end of the period 27,339 published articles.

and (3) multi-sensor and multi-temporal remote sensing for quantifying the impacts of environmental changes (deforestation, fire, droughts) on tropical forest canopies.

2. RADAR REMOTE SENSING FOR ESTIMATING TROPICAL FOREST STRUCTURE AND BIOMASS

Amazonian tropical forests are structurally complex and carbon-rich ecosystems, due to the size–frequency distribution of trees (CLARK; CLARK, 2000) and the three-dimensional arrangement of canopy (leaves, branches, trunks) from the superior strata to the ground (RICHARDS, 1996). The availability of light, humidity and constantly high temperatures influence the biological processes that control tree recruitment, competition, and growth rates (NICOTRA *et al*., 1999). One of the key variables that is influenced by this floristic and structural complexity is the forest aboveground biomass (AGB), in both horizontal and vertical gradients. Furthermore, this forest complexity is also related to disturbance intensity and spatial heterogeneity driven by edaphic and geomorphometric features of the landscape (CLARK; CLARK, 2000). Understanding forest structure variation and estimating forest biomass at regional and global scales by performing wall-to-wall mapping of the landscape are critical elements to provide information on the role of forests in determining the magnitude of terrestrial carbon flux, caused by deforestation or fragmentation processes, and their contribution to global climate change.

Remote sensing, in the forest biomass mapping context, has a critical role because many of the forest attributes of interest are retrievable at varying accuracy levels with a cost-effective value. Forest inventories assisted by remote sensing reap not only the benefits of producing results with lower cost and lesser time consumed than traditional methods, but also the advantage of conducting inventories in large forest areas or even sometimes life-threatening areas (HOU *et al.*, 2011). Optical remote-sensing systems (visible and infrared wavelengths) are limited in the tropics by cloud cover. However, new advances in microwave technologies can provide cloud-free data for mapping and forest monitoring and also for biomass estimate. It is interesting to note some possibilities and limitations of remote sensing data and methods, listed by Gibbs *et al.* (2007), which can support forest mapping and inventory at a national scale (Table 1).

Knowledge of the forest structure and the resulting biomass estimation can be obtained by indirect methods derived from remote sensing-based estimations, such as tree height, crown closure and stand types as major inputs. These variables are commonly used for estimating stand mean tree diameter and wood volume (KOCH, 2010). The wood volume can, subsequently, be multiplied by a biomass expansion factor for the final biomass estimation (CHÁIDEZ, 2009). For readers who are just beginning to learn about the applicability of remote sensing in forestry, the synergy between the use of laser scanning, known as Light Detection and Ranging (LIDAR) and Synthetic Aperture Radar (SAR) is discussed in Saatchi (2010) and Treuhaft *et al*. (2010). The synergy between multi- and hyperspectral data for forest biomass mapping is presented in an exhaustive overview by Koch (2010).

Within the range of sensor-products, this section focus on demonstrating how the specific remote sensing technology - RADAR - has been used as a tool for analyzing forest structure and estimating biomass in the Amazon. The physical principles of radar-interaction with the components of forest structure is very complex, especially in tropical forest areas, whose structure determines the scattering mechanisms of the incident radiation that hits the target and returns to the RADAR sensor. The content of leaves, branches and stems in the canopy as well as the ground are the components that produce scattering in forests. The interaction of the radar-signal with the targets and the consequent response received by the sensor also depends on the wavelength, polarization, and angle of incidence. According to Koch (2010), for forest cover mapping and biomass estimations, three basic approaches based on SAR data are used: backscatter, coherence, and phase-based approaches. One should remember that there are certain effects in the relationship between radar-signal and structural components of the forest stand, such as roughness of targets and humidity content, which should also be considered in the analysis. The SAR interferometric

Table 1: Benefits and limitations of remote sensing data to forests structure and biomass studies

Products	Description	Benefits	Limitations	Uncertainty
Optical remote sensors	• Uses visible and infrared wavelengths to measure spectral indices and correlate to ground based forest biomass measurements. Ex: Landsat, AVNIR/ALOS, HRV/SPOT, MODIS	• Satellite data routinely collected and available at regional and/or global scale • Regionally and/or globally consistent	• Limited ability to develop good models for tropical forests • Spectral indices saturate at relatively low C stocks • Can be technically demanding	• High
Very high-resolution optical remote sensors	Uses very high resolution images to measure tree height and crown area and allometry to estimate biomass stocks • Ex: 3D digital aerial imagery, IKONOS, QuickBIRD.	• Reduces time and cost of collecting forest inventory data • Reasonable accuracy • Excellent ground verification for deforestation baseline	• Only covers small areas (10 000s ha) • Can be expensive and technically demanding • No allometric relations based on crown area are available	• Low to medium
Radar remote sensors	• Uses microwave signal to measure forest vertical structure • Ex: ALOS/PALSAR-2, RADARSAT-2, COSMOSkyMed, TanDEM/TerraSAR-X.	• Satellite data are generally free • Can be accurate for open or sparse primary forest and secondary succession	• Less accurate in complex canopies of mature tropical forests because signal saturates • Mountainous terrain also increases errors • Can be expensive and technically demanding	• Medium
Laser remote sensors	• LiDAR uses laser light to estimates forest height/vertical structure • Ex: Structure and biomass 3-D satellite system combines Vegetation canopy LiDAR (VCL) with horizontal imager	• Accurately estimates full spatial variability of forest carbon stocks • Potential for satellite based system to estimate global forest carbon stocks	• Airborne-mounted sensors only option • Requires extensive field data for calibration • Can be expensive and technically demanding	•Low to medium

techniques, such as repeat–pass or single pass interferometry (InSAR) and polarimetric interferometry (PolInSAR), can also provide detailed information about three-dimensional forest structure of the scattering targets under study (TREUHAFT *et al*., 2009).

Some work in tropical areas show the proven applicability of radar (HOEKMAN; QUINONES, 2000; SANTOS *et al*., 2003; GONÇALVES *et al*., 2011; and SAATCHI *et al*., 2011), explaining the contributions of coherent and incoherent polarimetric attributes of forest structure complexity, when modeling forest volume or biomass. In turn, Pope *et al.* (1994) developed indices based on ratios and normalized differences of multi-polarimetric data using backscattering values (σ°) of horizontal (HH), vertical (VV) and cross polarizations (HV), which can be related to certain characteristics of vegetation cover, such as biomass index [BMI = $(\sigma^\circ_{HH} + \sigma^\circ_{VV}) / 2$], canopy structure index [CSI = $\sigma^\circ_{VV} / (\sigma^\circ_{VV} + \sigma^\circ_{HH})$], or volume scattering index [VSI = $\sigma^\circ_{HV} / (\sigma^\circ_{HV} + BMI)$], with important use in studies of tropical forests with radar data.

A first step in understanding the variability of forest structure is through the radar polarimetric signature (VAN ZYL *et al.,* 1987), where the polarization states of the electric fields E_v (vertical polarization) and E_h (horizontal polarization), which are associated with the radar backscatter (σ) and the dependence of the amplitude on the polarization mode, can be represented graphically as a function of ellipticity (χ) and orientation (ψ) angles of the transmitted wave, defining a three-dimensional surface plot called a polarization response (SANTOS *et al*., 2009) (Figure 2a, b, c). Density of trees, regular spatial distribution of trees, trunk diameter, density of twigs and branches, the moisture content of the leaves and soil types as well as dielectric constant of targets are some variables that influence this polarimetric behavior, whose signatures also show variations as a function of radar frequency and/or local incidence angle.

For modeling forest biomass through full-polarimetric SAR information, the attributes are classified into incoherent and coherent categories. The incoherent attribute types are based on information from the real part of each pixel. They are represented by the backscatter coefficient ($\sigma°$); the ratio of parallel polarization (Rp), the ratio of cross polarization (Rc), the total power (PT), reported by Woodhouse (2006); and also by the indices for forest environments, formulated by Pope *et al*. (1994), named as the biomass index (BMI), the canopy structure index (CSI) and the volume scattering index (VSI). The coherent attributes are derived from SAR phase-information (HENDERSON; LEWIS, 1998), which are represented by polarimetric coherence of HH-VV (γ) and phase difference of HH-VV ($\Delta\varphi$). Furthermore, we analyzed the parameters resulting from the decomposition by coherence matrix [T], defined as entropy (H), anisotropy (A) and the mean alpha angle ($\overline{\alpha}$) (CLOUDE; POTTIER, 1997); the magnitude (αs) and Touzi phase ($\Phi\alpha s$), also derived from the same former decomposition (TOUZI, 2007). Additionally, we considered the orientation angle (ψ) and heliticity (τ_m), derived from two stages: (1) the Graves matrix [G]; and (2) the Kennaugh-Huynen matrix, described in Touzi *et al*. (2009). Also, the volume scattering components (Pv), double bounce (Pd) and surface (Ps), resulting from the decomposition matrix [C], according to Freeman and Durden (1998).

To show the full-polarimetric capability in the estimate of tropical primary and secondary forest biomass, one example is the model developed by Narvaes (2010), which tested a number of attributes (Figure 3a) derived from ALOS/PALSAR images that, following statistical criteria, defined the best performance model (Equation 1):

$$[AGB = -\ 1221.37 - 70.31\ (\sigma°_{HH}) + 1064.65\ (P_V) + 6.28\ (\alpha_{S2}) - 2.42\ (\Phi_{S2}) + 3.44\ (\Phi_{S3}) + 6.05\ (\tau_m)]\ \ldots.. \quad (1)$$

Where: $\sigma°_{HH}$ is the backscatter coefficient at HH polarization; P_V is the volume scattering component of Freeman's decomposition; α_{S2} is the Touzi's magnitude of medium scattering; Φ_{S2} and Φ_{S3} are the Touzi's phase of the medium and low scattering, respectively; and τ_m is the helicity mean angle.

The selected attributes demonstrate the importance of radar phase information to estimate the biomass of primary and secondary forests. The biomass estimation error of the predictive model mentioned above is around 8%, based on independent sampling blocks used for the validation (Figure 3b).

The case cited above reports the use of polarimetry. However, the modeling of biomass from radar interferometry techniques has also been a very broad field of research and applicability, as shown by Neeff *et al*. (2003), Kugler *et al*. (2006) and Treuhaft *et al*. (2010). Interferometry approach is indicated for tropical areas because forests, generally, have a high biomass content; thus the possible saturation effect of the radar-signal is minimal compared to the simpler techniques of polarimetry.

An alternative approach to extract forest structural information from radar interferometry is based on tomography technique (CLOUDE; PAPATHANASSIOU, 2008), where a real 3D imaging of the scene is acquired by creating an additional synthetic aperture layer containing information on elevation. This technique uses a coherent combination of images obtained from multiple baselines of flight tracks. However, researches in this field of radar tomography for tropical forests are in the early stages (CLOUDE *et al*., 2009; LOMBARDINI *et al*., 2012; DINH *et al*., 2013).

3. MULTI-TEMPORAL OPTICAL REMOTE SENSING FOR ANALYZING PHENOLOGICAL PATTERNS

3.1 Land surface phenology

Phenology is a key component for monitoring terrestrial ecosystem changes in response to climatic variations on short and long time scales (HMIMINA *et al*., 2013; LIANG *et al*., 2011). Vegetation phenology is important because it affects terrestrial carbon cycling at different ecosystems and climate

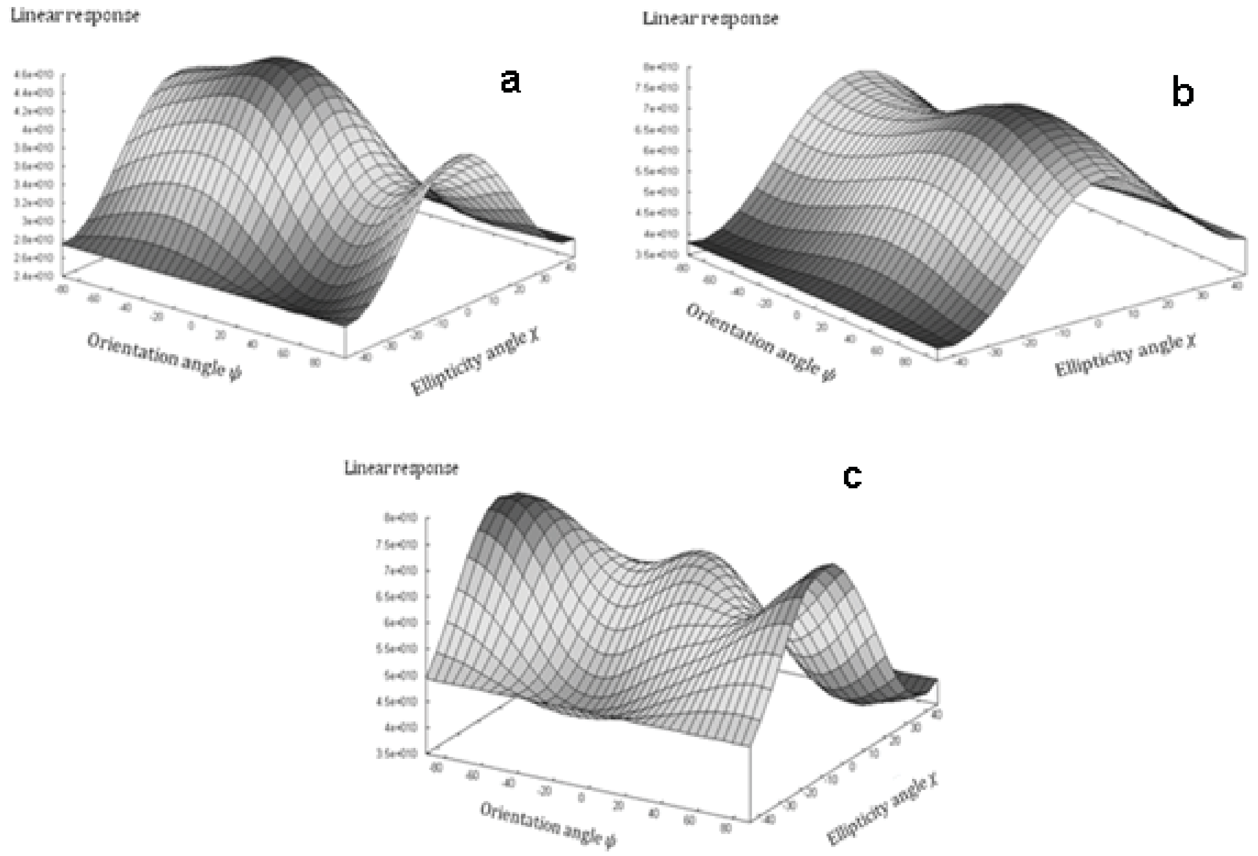

Fig. 2 - PALSAR/ALOS polarimetric behaviour of (a) primary forest (b) forest with timber exploitation, and (c) intermediate secondary succession in the Amazonian region.

regimes; eco-physiological and hydrologic processes; and land-atmosphere interactions (GANGULY *et al*., 2010; HEIMANN *et al*., 1998). Phenological observations over tropical forests are generally carried out using two main approaches: (1) surface observations and (2) orbital optical remote sensing (MELAAS *et al*., 2013). Both approaches have their advantages and disadvantages. By using traditional ground observations, detailed phenology metrics are obtained for individual plants or species. These metrics cannot be captured by remote sensing that aggregate phenological information at the spatial resolution of the whole canopy as observed by sensors onboard of satellites. On the other hand, field observations of vegetation phenology are punctual, expensive and time consuming, providing only little information on the spatial variability of timing of phenological events (SOUDANI *et al*., 2012). Because of the limited number of field-based phenological studies in tropical forests, remote sensing, due to the high temporal data acquisition and large area coverage, is still the best alternative for large-scale monitoring of phenology. However, uncertainties in data processing and pixel quality control for noise reduction in satellite data time series can affect the correct identification of vegetation phenological markers (VERBESSELT *et al*., 2010; SOUDANI *et al*., 2012). Noise is generally a result of atmospheric effects and variable Sun-viewing geometry.

"Land surface phenology", which is distinct from the traditional definition of phenology, is a term that has been used to represent the seasonal pattern of variation in vegetated land surfaces observed from remote sensing (TAN *et al*., 2011). The sensor that best represent the state-of-art of land surface phenology is the Moderate Resolution Imaging Spectroradiometer (MODIS), on board Terra and Aqua satellites. Since 2000, MODIS has provided an excellent basis for regional-to-global scale land surface phenological studies (AHL *et al*., 2006; ZHANG *et al*., 2006; GANGULY *et al*., 2010). MODIS presented significant improvements in terms of spectral resolution (36 spectral bands), spatial resolution (250 m for bands 1-2; 500 m for bands 3-7; 1 km for bands 8-36), geolocation accuracy (50 m at nadir), calibration, and data processing

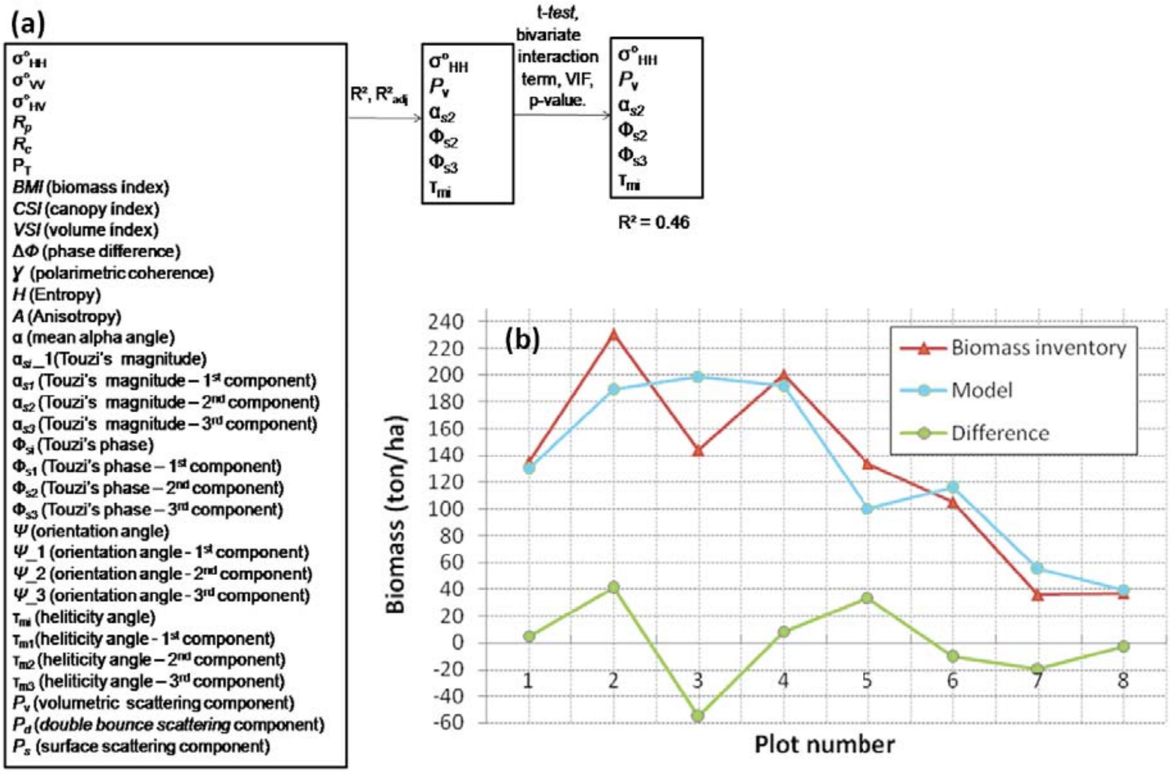

Fig. 3 - ALOS/PALSAR polarimetric attributes tested to construct the model (a) and performance of aboveground biomass model compared from the field measured in the independent sampling blocks (b).

for atmospheric correction and cloud screening (HMIMINA *et al*., 2013). At the orbit of 705 km, MODIS uses a large field-of-view (FOV) of ±55º to obtain a 2,330-km swath and to provide global coverage every one to two days. For land surface phenology studies using MODIS, products based on vegetation indices (VIs) are generally used. Two MODIS products can be highlighted: (1) the VIs products that include more specifically the Normalized Difference Vegetation Index (NDVI) and the Enhanced Vegetation Index (EVI); (2) the Global Land Cover Dynamics (MLCD) product, which is based on the EVI and is informally called the "MODIS Global Vegetation Phenology product".

3.2 MODIS Vegetation Indices products

In relation to the first and most commonly used approach in tropical forests, spatial and temporal variations in NDVI and EVI are operationally derived at 16-day and monthly intervals from the Terra and Aqua satellites for seasonal and inter-annual monitoring of the vegetation. The EVI was proposed by Huete *et al*. (2002) to reduce atmospheric and soil background influences on the NDVI and to have improved sensitivity over high biomass regions (less signal saturation with increasing Leaf Area Index (LAI)). Data for both VIs can be analyzed at 250 m, 500 m, 1 km and 0.05° spatial resolutions (e.g., the product MOD13Q1 MODIS/Terra Vegetation Indices 16-Day L3 Global 250-m SIN Grid V005).

The use of compositing VIs products instead of daily data is due to two main reasons. First, when compared to nadir-viewing instruments, large FOV sensors like MODIS have the advantage of increasing spatial and temporal coverage. On the other hand, because of the anisotropy of vegetation, the off-nadir viewing introduces changes in sensor signal in response to variations in Sun-viewing geometry (GALVÃO *et al*., 2011). In short, strong reflectance differences not associated with canopy photosynthetic activity or phenology can be registered by MODIS at the bands used for VIs determination between consecutive days (BREUNIG *et al*., 2011). The resulting directional effects are target and wavelength dependent. As a consequence of this spectral dependence, these effects are not completely removed by the determination of VIs.

Second, atmospheric effects (e.g., molecular scattering, absorption, and aerosols), including cloud cover, introduce large uncertainties on VIs determination. Thus, atmospheric correction is essential to support phenologic studies. Compositing schemes try to select the highest quality pixels in the compositing period for more precise time-series analysis. For land surface phenology, an important question is how to shorten the compositing period to look for better phenologic markers without adding more uncertainties in time series analysis. MODIS data have been frequently reprocessed and there were significant improvements with the transition from Collections 4 to 5. Maybe the answer for this question and for the other current issues relies on future improvements in atmospheric and bidirectional reflectance distribution function (BRDF) correction procedures and in small adjustments on VIs formulation.

Even using VIs from 16-days compositing schemes, atmospheric conditions are critical in some regions of the Amazon for land surface phenology. However, a very nice aspect of the MODIS VIs products is that they provide all the necessary information for a detailed analysis of NDVI and EVI on a per pixel basis, including the pixel quality retrievals, the input surface reflectance of the bands used to generate the VIs, and the angles describing the Sun-viewing geometry during data acquisition.

An example of the pixel reliability images retrieved for some compositing periods of 2001 over the Tapajós National Forest, located in the Brazilian state of *Pará*, is illustrated in Figures 4a-f. Good data (code zero), marginal data (code 1) and cloudy data (code 3) for the different Days of Year (DOY) are represented by red, green and yellow colors, respectively. Code 2 is obviously not represented because it refers to targets covered with snow/ice. Results of Figure 4 were extracted from the MOD13Q1 product (MODIS/Terra Vegetation Indices 16-Day L3 Global 250-m SIN Grid V005) and refer only to the area within the limits of the Tapajós forest (Figure 4a). From the inspection of Figure 4, we observed that the uncertainties were larger in the rainy season (December to May) due to the more frequent cloud cover (predominance of yellow color or code 3 in Figure 4b). They decreased towards the dry season (June to November), as expected. However, except for the DOY 209 (July 27, 2001), having all pixels of the Tapajós forest in red color (code zero in Figure 4d), the uncertainties were still present in the dry season of the Tapajós region, as indicated by the presence of green (marginal data) and yellow (cloudy data) colors in the other dates.

In Table 2, a detailed analysis showed that the high percentages of good data (code zero) were observed in the dry season only for two dates between July and August of 2001 (DOYs 209 and 225 with 100% and 59% of good pixel retrievals, respectively). The other compositing dates in the rainy and dry seasons were dominated by cloudy (code 3) or marginal (code 1) data. The latter data require further inspection for other quality assurance information to reduce uncertainties in data analysis.

Cloudy data in the rainy season does not generally allow a reliable analysis of the VIs behavior from December to May in the Tapajós region. Despite the uncertainties in pixel quality retrievals, when using only pixels having codes zero or 1 (good or marginal data) for a small portion of the Tapajós forest (red square in Figure 4a; 9 x 9 pixels), an increase in EVI was observed along the dry season (June-November) over seasonal semi-deciduous forest (Figure 5). In reality, only two dates had pixels with zero code for this portion of the scene (green symbols in Figure 5). From June to November, NDVI presented much smaller variation because it is saturated at high LAI values (results not shown). According to Huete *et al*. (2006), the EVI increase in the sunnier dry season in tropical Amazonian forest may indicate that sunlight have more influence than rainfall in the phenology of these forests. As pointed out by Bradley *et al*. (2011), the majority of the Amazonian Terra Firme forest appears to have radiation as the driver of phenology.

In the literature, much of the studies assessing the phenologic variability of the Amazonian tropical forests have been devoted to understand the unexpected behavior of EVI along the dry season and, especially, in response to severe droughts (inter-annual variations). For example, when compared to non-drought years, Saleska *et al*. (2007) reported an increase in greenness for the 2005 drought, as expressed by higher EVI values over the Amazon, as opposed

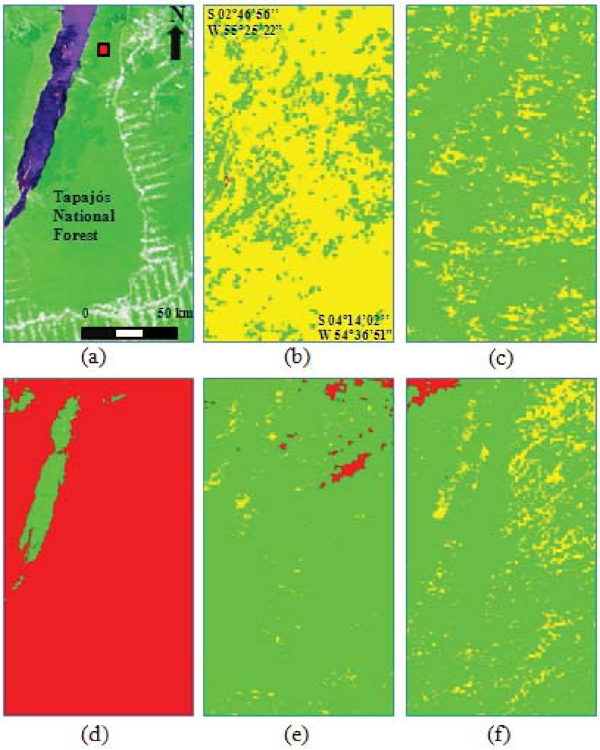

Fig. 4 - (a) MODIS color composites from the 16-days and 250-m MOD13Q1 product at the Tapajós region with the bands at red, near infrared and blue wavelengths in red, green and blue colors, respectively. Pixel reliability images are shown for different dates in 2001 in (b) January 1; (c) May 8; (d) July 27; (e) September 13; and (f) November 16. In (b)-(f), good (code zero), marginal (code 1) and cloudy (code 3) data are represented in red, green and yellow colors, respectively. The red square in (a) indicates a portion of the image over seasonal semi-deciduous forest (81 pixels; 9 x 9 pixels) used to obtain Figure 5.

to field-based estimates of decreasing plant productivity and tree mortality (PHILLIPS *et al*., 2009). On the other hand, Xu *et al*. (2011) observed a widespread decline in photosynthetic activity for the 2010 drought (lower EVI values). Nice literature reviews on the potential causes of the unexpected green-up of vegetation with droughts, reported by Saleska *et al*. (2007), have been published by Asner and Alencar (2010) and by Anderson (2012). As summarized by Moura *et al*. (2012), the possible causes cited in the literature for the contradictory findings about the tropical forest resilience to droughts include factors such as: leaf flush at the top of the canopy; changes in LAI; modifications in canopy structure associated with tree mortality; diurnal variability in leaf water; and clouds and aerosol effects (ANDERSON *et al*., 2010; BRANDO *et al*., 2010; SAMANTA *et al*., 2010).

Even the intra-annual EVI variations reported by Huete *et al*. (2006) are not completely understood. Galvão *et al*. (2011) have shown that the EVI is strongly dependent on the near infrared reflectance and is much more sensitive to solar illumination, view angle and view direction than the NDVI. While solar illumination is a source of intra-annual dry season EVI variability, view angle and view directions are sources of inter-annual variability of this index (MOURA *et al*., 2012; GALVÃO *et al*., 2013). These controversial findings show that validation of detectable MODIS satellite phenologic patterns, using surface observations and other better spatial resolution sensors, is still necessary.

3.3 MODIS Global Vegetation phenology product

The Collection 5 MODIS Global Land Cover Dynamics (MCD12Q2) provides combined information from the Terra and Aqua related to spatiotemporal dynamics in land surface phenology product at a spatial resolution of 500 m and at 8-day input data. As discussed by Ganguly *et al*. (2010), the MLCD algorithm described in Zhang *et al*. (2006) represents vegetation growth cycles using four transition dates estimated from time series of MODIS EVI: (1) green-up: the date of onset of EVI increase; (2) maturity: the date of onset of EVI maximum; (3) senescence: the date of onset of EVI decrease; and (4) dormancy: the date of onset of EVI minimum. When compared to the conventional EVI described in the previous section, the EVI from the MLCD is computed from MODIS nadir bidirectional reflectance distribution function (BRDF)-adjusted reflectance (NBAR) data. The objective of this adjustment is to model reflectance values as if they were acquired from nadir view (SCHAAF *et al*., 2002). The view angles effects on the EVI are then minimized in NBAR data.

According to Ganguly *et al*. (2010), the MLCD results are less reliable for tropical evergreen forests than for other ecosystems with predominance of deciduous forests. In tropical regions, there is a need to provide better characterization of the errors and uncertainties

Table 2: Pixel reliability from the 16-days and 250-m MOD13Q1 product indicating the percentage of good (code zero), marginal (code 1) and cloudy (code 3) data in the year of 2001 over the brazilian Tapajós national forest. The dry (June-November) and rainy (December-May) local seasons are indicated

	Day of Year (DOY)																							
Code	Rainy Season										Dry Season in the Tapajós Region										Rainy Season			
	1	17	33	49	65	81	97	113	129	145	161	177	193	209	225	241	257	273	289	305	321	337	353	365
0	0	0	0	0	2	0	0	0	0	0	14	18	14	100	59	4	1	1	0	0	0	0	1	0
1	17	52	47	18	61	28	13	71	82	91	41	80	86	0	41	96	98	99	96	99	91	61	92	5
3	83	48	53	82	37	72	87	29	18	9	45	2	0	0	0	0	1	0	4	1	9	39	7	95
Total (%)	100	100	100	100	100	100	100	100	100	100	100	100	100	100	100	100	100	100	100	100	100	100	100	100

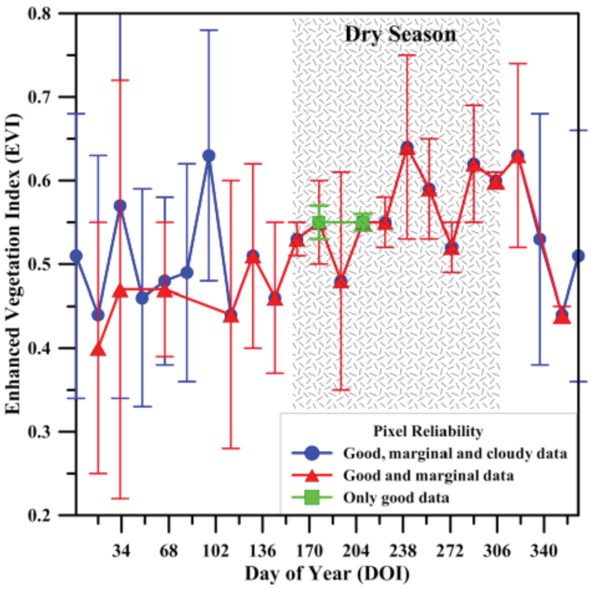

Fig. 5 - Average and standard deviation MODIS EVI values over seasonal semi-deciduous forest of the Tapajós National Forest (red square of 9 x 9 pixels in Figure 1a) using different quality retrieval pixels from the reliability image. Good data (zero code) were observed only in two dates. The 2001 dry season is indicated.

associated with MLCD results, to develop improved methods for pre-processing input data, and to understand the nature and utility of the retrieved phenological metrics. Except for the tropics, when compared with field observations in North American test sites, the authors showed that retrieved transition dates from the MLCD were generally realistic. However, on these North American sites, larger uncertainties were observed at the end of season metrics associated with vegetation senescence and dormancy than at the start of season metrics.

Recently, the TIMESAT software (GAO *et al*., 2008) was modified by Tan *et al*. (2011) to retrieve phenology metrics based on MODIS time series of EVI and NDVI calculated from 8-days compositing Terra surface reflectance products at 250 m and 500 m spatial resolutions. Derivative analysis preceded by Savitzky–Golay filtering was applied to define key phenology dates and to retrieve a set of phenology metrics, which were compared with ground phenology observations over North America. Tan *et al*. (2011) discussed the difficulties to validate MODIS phenology metrics due to the scale-mismatch with ground observations. According to them, results over North America showed also the need of additional analysis to define the best VI (EVI or NDVI) to represent the phenologic metrics due to the lack of agreement between the indices.

3.4 From moderate spatial resolution data to punctual field phenological observations

Validation is essential for calibrating remote sensing based scientific algorithms. MODIS products are available at a range of spatial scales, whereas field measurements are punctual. Thus, there is a constant need for data sets and methods that link ground-based observations of phenology to moderate spatial resolution land surface phenology products (MEELAS *et al*., 2013). The use of better spatial and spectral resolution airborne and satellite sensors is very important to address the scaling issue for MODIS validation (MORISETTE *et al*., 2002). In this context, a 30-year time series of Landsat images cannot be ignored in land surface phenology studies (MEELAS *et al*., 2013). Furthermore, constellation of satellites (e.g., RapidEye) that allows us to acquire high spatial resolution data with more frequent revisit time is another possibility. Such sensors better sample the tropical forest heterogeneity, but off-nadir viewing (pointing instrument capability) should be considered with care in data analysis of VIs. Although still acquiring punctual measurements, tower-based digital cameras and instruments that track local seasonal variations in VIs or in vegetation phenology can also be helpful (RICHARDSON *et al*., 2007; SOUDANI *et al*., 2012).

Imaging Spectroscopy (hyperspectral remote sensing) comprises the simultaneous acquisition of spatially co-registered images, in many narrow, spectrally contiguous bands. From airborne level of data acquisition, when combined to LiDAR, imaging spectrometers can be used to relate phenological variation to micro-topography, derived from fine scaled digital elevation models (DEMs), and to simultaneous measurements of vegetation structure (ASNER *et al*., 2012; SCHAEPMAN *et al*., 2009). From orbital level, the combined use of MODIS/Terra and Hyperion/Earth Observing One (EO-1) has contributed to improve the understanding of the phenologic variability in the Amazonian tropical forest (HUETE *et al*., 2008; GALVÃO *et al*., 2011).

Since 2000, Hyperion has been acquiring images in 196 calibrated bands (10 nm of bandwidth) in the 426–2395 nm range with a spatial resolution of 30 m and a swath width of 7.7 km. The 16-day revisit time can be reduced by cross-track pointing to obtain time series of VIs during the dry season of tropical forests. Data can be obtained with different view angles (nadir and off-nadir) and directions (forward scattering and backscattering) (GALVÃO *et al*., 2011). Thus, when analyzing time series of Hyperion VIs, it is necessary to take into account the potential influence of the geometry of image acquisition on data variability (GALVÃO *et al*., 2013).

An example using Hyperion EVI is presented in Figure 6 for the seasonal evergreen forest of the Brazilian *Mato Grosso* state. Higher EVI values were observed in the backscattering mode (squares) than in the forward scattering direction (stars) due to the predominance of sunlit canopy components for the sensor (higher near infrared reflectance). In the backscattering direction, EVI increased also with large view zenith angles. However, at Hyperion nadir viewing (circles in Figure 6), EVI increased towards the end of the dry season in agreement with the MODIS EVI behavior observed in the study area (results not shown). Galvão *et al*. (2011) associated this behavior with the strong near infrared dependence of EVI, with the decrease in solar zenith angle (SZA) and with the reduction in canopy shadows viewed by the sensors towards the end of the dry season.

Besides the conventional EVI and NDVI, hyperspectral instruments allow the calculation of several narrowband VIs that can be used to measure vegetation properties associated with structure (e.g., green leaf biomass; LAI), canopy biochemistry (e.g., pigments; moisture) and plant physiology (e.g., water stress) (ROBERTS *et al*., 2012; GALVÃO *et al*., 2013). Some hyperspectral VIs with equations and references are shown in Table 3 but a more complete list was presented and reviewed by Roberts *et al*. (2012). Because they are calculated from bands positioned at different spectral regions and have different sensitivity to view-illumination effects, time series of distinct hyperspectral VIs can be used to reduce MODIS EVI uncertainties in the

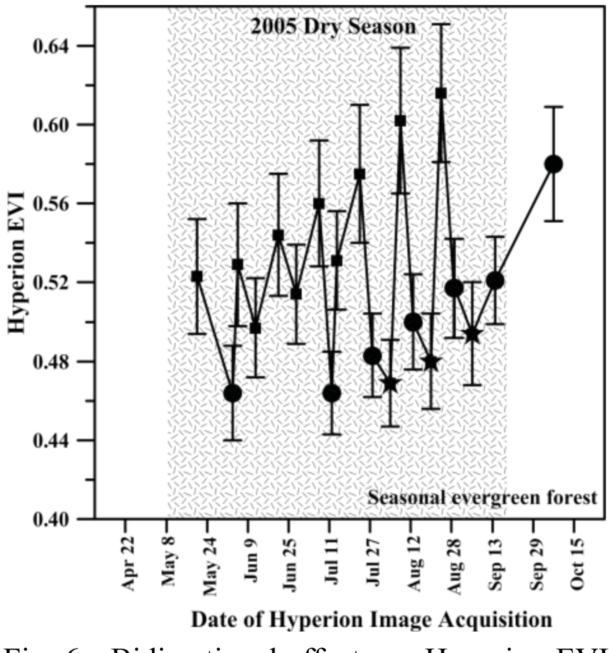

Fig. 6 - Bidirectional effects on Hyperion EVI of the Seasonal Evergreen Forest in the 2005 dry season for a study area located in the Mato Grosso state. Average and standard deviation EVI data calculated from nadir viewing (500 pixels) are indicated by circles. Squares and stars indicate off-nadir viewing in backscattering and forward scattering directions, respectively.

Table 3: Examples of some narrow-band vegetation indices that can be calculated from hyperspectral data

Vegetation Index	Formula [a]	Reference
Enhanced Vegetation Index (EVI)	2.5*((ρ864 - ρ671)/(ρ864 + 6* ρ671 – 7.5* ρ467 + 1))	Huete *et al*. (2002)
Normalized Difference Infrared Index (NDII)	(ρ823 – ρ1649)/(ρ823 + ρ1649)	Hunt and Rock (1989)
Normalized Difference Vegetation Index (NDVI)	(ρ864 - ρ671)/(ρ864 + ρ671)	Rouse *et al.* (1973)
Normalized Difference Water Index (NDWI)	(ρ854 – ρ1245)/(ρ854 + ρ1245)	Gao (1996)
Photochemical Reflectance Index (PRI)	(ρ529 – ρ569)/(ρ529 + ρ569)	Gamon *et al.* (1997)
Red Edge NDVI (RENDVI)	(ρ752 – ρ701)/(ρ752 + ρ701)	Gitelson *et al.* (1996)
Structure Insensitive Pigment Index (SIPI)	(ρ803 – ρ467)/(ρ803 + ρ681)	Penuelas *et al.* (1995)
Visible Atmospherically Resistant Index (VARI)	(ρ559 – ρ640)/(ρ559 + ρ640 - ρ467)	Gitelson *et al.* (2002)
Visible Green Index (VIg)	(ρ559 – ρ640)/(ρ559 + ρ640)	Gitelson *et al.* (2002)
Vogelmann Red Edge Index (VOG)	ρ742/ρ722	Vogelmann *et al.* (1993)

assessment of phenologic variability along the dry season of tropical evergreen forests.

4. MULTI-SENSOR AND MULTI-TEMPORAL REMOTE SENSING FOR QUANTIFYING THE IMPACTS OF ENVIRONMENTAL CHANGES

As discussed above, quantifying spatial and temporal variation of biomass and phenological cycles of Amazonian forest is critical for analyzing the magnitude, seasonal cycle and direction of carbon fluxes between the biosphere and atmosphere. However, both carbon stocks and fluxes are exposed to natural and human-driven disturbances or changes that can directly impact the Amazon biome carbon balance. In this section, we first present an overview about the causes and consequences of environmental changes in Amazonia. This section is followed by case studies demonstrating the quantification of the changes and impacts using currently available remote sensing technology and data.

4.1 Environmental changes in Amazonia

Remote sensing has been a key tool since mid 80s to detect environmental changes in Amazonia. The most pervasive changes are related to deforestation, degradation and fires. Moreover, with climate change, increased frequency of droughts is becoming especially critical. Global climate models (GCMs), have been predicting increased drought probability in the region (LI *et al*., 2006, IPCC, 2007).

Historically, deforestation has been removing around 0.14 and 0.26 Pg C yr-1 over the decades of 1980 and 1990, respectively (HOUGHTON *et al*. 2000, DEFRIES *et al*. 2002). Monitoring using Landsat imagery have demonstrated that annual deforestation rates, have been drastically reduced from 17,562 km^2 yr^{-1} (mean between 1988 and 2004) to 4,571 km^2 deforested in 2012 according to INPE/PRODES. Despite very uncertain yet, selective logging and forest fire also contribute for increasing the deforestation impact. Studies using Thematic Mapper (TM) and Enhanced Thematic Mapper Plus (ETM+) optical sensors onboard of Landsat family satellites and MODIS sensor have demonstrated their capability to estimate burned area in Amazonia. During the 1997/1998 severe El Niño event, Alencar *et al*. (2006) estimated a total of 26,000 km^2 of forests burned forest using Landsat imagery. This area burnt equates to a committed gross carbon emissions varying between 0.024 and 0.165 Pg C. Moreover, using MODIS data, Morton *et al*. (2013) estimated that forest fires burned around 85,500 km^2 of southern Amazonian forests between 1999 and 2010.

Climate variability, leading to droughts is also a major factor influencing the biomass and carbon dynamics in Amazonia. In the orbital remote sensing Era the Amazon was affected by at least three severe drought events mainly related to the El Niño Southern Oscillation (ENSO) phenomenon in 1982/1983, 1986/1987 and 1997/and two associated to sea surface temperature anomalies occurring in the tropical north Atlantic in 2005 and 2010, perhaps linked to the Atlantic Multidecadal Oscillation (AMO) (MARENGO *et al*., 2011). Both events tend to reduce rainfall in Amazonia, with the north and eastern flanks of the region being more affect by the ENSO and the southern and western being more affected by the AMO (SAATCHI *et al*., 2013). Intensification of drought impacts normally occurs by the association with fires and deforestation (COCHRANE; LAURANCE, 2008, HUTYRA *et al*., 2005, ARAGÃO *et al*., 2008, MALHI *et al*., 2008).

The multitude of sensors, with wavelengths ranging from visible (0.4 x 10^{-6} – 0.7 x 10^{-6} m) to microwave (1.0 x 10^{-2} m – 1.0 m) has recently enhanced our capacity to detect, monitor and quantify the impacts of droughts in Amazonia. For instance, Aragão *et al*. (2007) using rainfall data from the Tropical Rainfall Measuring Mission (TRMM) satellite showed that an area of 3,300,000 km^2 was impacted by water deficit during the 2005 drought. The stressed area was strongly related to tree mortality in the region (PHILLIPS *et al*., 2009) and with a 33% increase in fire incidence (ARAGÃO *et al*., 2007). The water stress has also been related to anomalies in vegetation indices related to changes in the structure and photosynthetic capacity of the canopy (SALESKA *et al*., 2007). It is clear that alone, both human- or climate-induced changes are able to disrupt the stability of the system. Critically important, though, are the feedbacks between these two pathways of disturbance. Spracklen *et al*. (2012) demonstrated using data from MODIS and an atmospheric transport model that deforestation can significantly reduce rainfall in Amazonia. This means that deforestation is likely to exacerbate the impacts of natural climate variability in the region, with consequences for the function of Amazonia.

Here we presented an overview of the impacts of environmental changes measured by satellite. In the next section, we will explore some of the remote sensing technology available and applications in more detail.

4.2 Mapping deforestation and degradation

Since early 1990s, quantification of deforestation rates in Amazonia using Landsat imagery and digital image processing techniques (e.g. SKOLE; TUCKER, 1993, SHIMABUKURO *et al*., 1998, HOUGHTON *et al*., 2000) has become an important field of research within the remote sensing community. Among several techniques used, one of the most popular is the application of the spectral mixture analysis, which estimate sub-pixel fraction of different components contributing to the spectral response of the pixel in a multi-spectral dataset (SHIMABUKURO *et al*., 1998). The usage of this simple concept increased rapidly because of its capacity to reduce the dimensionality of the multi-spectral dataset and accurately discriminate different land uses from tropical vegetation (e.g. ADAMS *et al*., 1995, SHIMABUKURO *et al*., 1998, LU *et al*., 2003). Technically speaking, the spectral mixture model can be defined as a linear combination of the spectral response of each component within a pixel in a given spatial resolution. This mixture will determine the pixel value in each spectral band. To decompose the pixel into its component fractions, we can assume that (Equation 2):

$$R_i = \sum_{k=1}^{n} f_k R_{ik} + \varepsilon_i \qquad (2)$$

where i is the number of spectral bands in the multi-spectral dataset, k is the number of components that contribute to the reflectance of the pixel (also known as endmembers), R_i is the reflectance value of band i of a given pixel. Each pixel contains one or more endmembers and f_k is the fraction of the endmember k within the pixel; R_{ik} is the spectral reflectance of endmember k within the pixel on band i, and ε_i is the associated error for band i. As f_k is the fraction of an endmember within the pixel, then the sum of all endmember fractions should be equal to 1 (Equation 3):

$$\sum_{k=1}^{n} f_k = 1 \qquad (3)$$

Moreover, f_k must be constrained between $0 \leq f_k \leq 1$.

By reducing dimensionality of multi-spectral Landsat data and retaining the fidelity of information in the images, application of this model increased the efficiency of segmentation procedure by using a single band as input (SHIMABUKURO *et al.*, 1998). This method was then used for the development of the world's oldest operational tropical deforestation monitoring system for the Brazilian Amazon (PRODES project). Following the experience with the Landsat data, and the availability of daily MODIS imagery, Anderson *et al.* (2005) proposed a similar method, using soil fraction images as the origin of INPE's deforestation detection in near real time project (DETER project), that provides monthly information about the deforestation rates in Amazonia (Figure 7).

The same concept has been used to quantify selective logging in Amazonia (ASNER *et al.*, 2004), fire (COCHRANE, 1998, ANDERSON *et al.*, 2005, SHIMABUKURO *et al.*, 2009, ALENCAR *et al.* 2011, MORTON *et al.*, 2011, LIMA *et al.*, 2012) or both (MATRICARDI *et al.*, 2010) from multiple optical satellite sources (Landsat, MODIS, SPOT). The study of selective logging and degradation, in general, is done by exploring the information contained in the non-photosynthetic active vegetation fraction, which is related to dead organic matter produced from the disturbance. Studies aiming to detect fires, on the other hand, tend to use the information in the shade fraction (e.g. SHIMABUKURO *et al.*, 2009).

One of the key applications of this technique is to extract quantitative information on the areal extent of forests burned. Applying the linear mixture model to MODIS/Terra daily surface reflectance data (MOD09 c4 product), Shimabukuro *et al.* (2009) showed that fire impacted a total area of 6,500 km^2, with 2800 km^2 corresponding to forest understorey fires. Figure

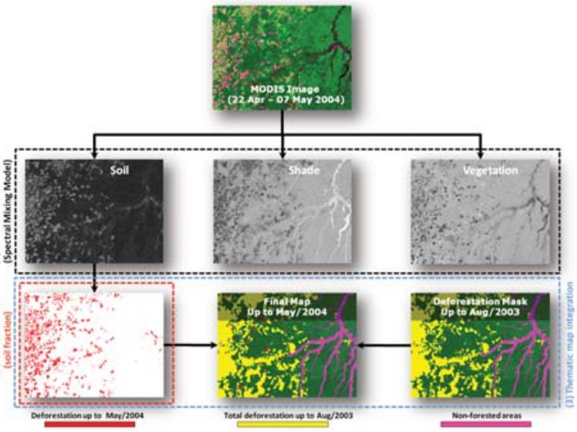

Fig. 7 - Workflow of the DETER methodology implemented for generating monthly deforestation rates. Specifically the method starts with application of the linear mixture model to decompose the per pixel information into its soil, shade and vegetation fractions (1), followed by the region growing segmentation and unsupervised classification of the segments (2) and finally, the process is completed by integrating the thematic map produced with information from previous deforested areas (3).

8 illustrates an example of the application of the spectral mixture model technique in MODIS images (Figure 8a) for mapping burnt scars enhanced in the shade fraction image (Figure 8b) and subsequent integration with deforestation data for extraction of understory fire information (Figure 8c).

Another critical point for discussion is the influence of droughts and how it can affect fire patterns and forest functioning. So, in the next section we compiled information of studies using multi-temporal remote sensing data for evaluating these impacts.

4.3 Mapping and quantifying anomalies in multi-temporal datasets

Droughts in Amazonia are characterized by a shortage of rainfall during the dry season, leading the forest ecosystem to water deficit (ARAGÃO *et al.*, 2007) and consequent water stress with negative implication for tree survivorship (PHILLIPS *et al.*, 2009). Several authors (e.g. ZENG *et al.*, 2008, XU *et al.*, 2010, ANDERSON *et al.*, 2010) used rainfall data from the Tropical Rainfall Measuring Mission (TRMM) product 3B43 monthly precipitation to study the extent and intensity of droughts that

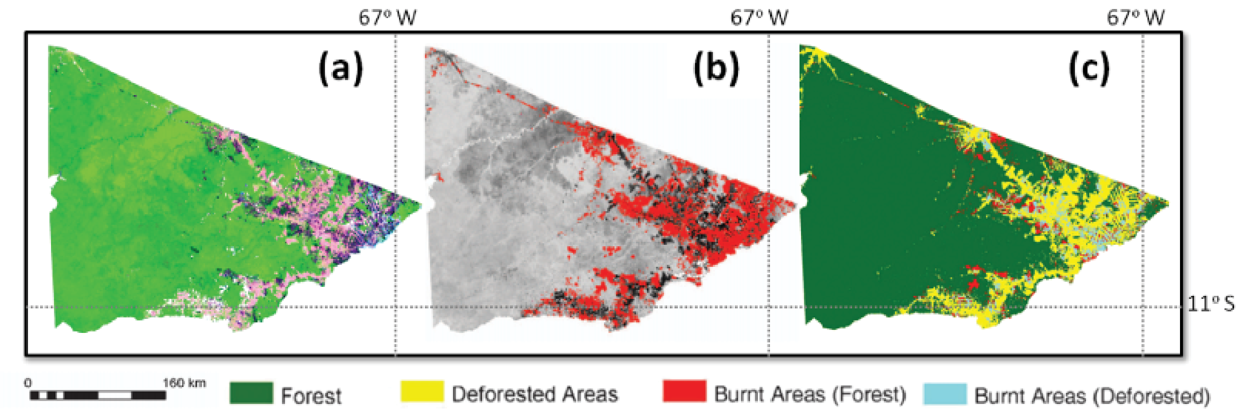

Fig. 8 - (a) Color composite of MODIS bands 6 (red channel), band 2 (green channel) and band 1 (blue channel). (b) Shade fraction image overlayed by the result of the classification of burnt areas and (c) same as (b) but overlayed with the forest/deforestation mask from PRODES project. Source: Modified from Shimabukuro et al. (2009).

occurred in Amazonia. The TRMM is a satellite with non-sun-synchronous equatorial orbit, with 350 km of altitude and 35° degrees inclination to the Equator designed to measure tropical rainfall, between 50° south to 50° north latitude (http://disc.gsfc.nasa.gov/precipitation/trmm_intro.shtml). This satellite carries onboard three instruments used to estimate rainfall: (1) the Precipitation Radar (PR), operating at a frequency of 13.8 GHz (wavelength ~ 2.2 cm); (2) the TRMM Microwave Image (TMI), which is a nine-channel passive microwave radiometer operating at frequencies ranging from 85.5 GHz (wavelength ~ 0.35 cm) to 10.65 GHz (wavelength ~ 2.8 cm); and (3) the Visible and Infrared Scanner (VIRS), which is a five-channel visible/infrared radiometer with wavelengths ranging from 0.63 µm to 12 µm. The 3B43 algorithm use TRMM sensors and other independent sources of data to produce monthly rainfall data (mm/hr) at a spatial resolution of 0.25° by 0.25°.

A common metrics to identify periods of time when rainfall is anomalously high or low in relation to the long-term observed temporal pattern is the calculation of z-scores. This metrics indicates the intensity and duration of anomalous periods in a time-series. So, for a dataset containing monthly data, for a given month, the anomaly (z-score) can be calculated as the departure of the specific month values from the mean long-term mean (*l_mean*) of the month, normalized by the standard deviation (σ) of the data. The monthly anomalies from the TRMM data ($TRMM_{anomaly}$) can, then, be calculated for each month (*t*) of a given year (*y*) in a pixel-by-pixel basis with latitude (*i*) and longitude (*j*) as (Equation 4):

$$TRMM_{anomaly,t}(i,j) = \frac{TRMM_{y,t}(i,j) - TRMM_{l\_mean,t}(i,j)}{\sigma_{l\_mean,t}(i,j)} \tag{4}$$

The information produced from this calculation allows the detection of spatially explicit deviations of rainfall values from the normal and the analysis of temporal changes in the anomalous patterns (Figure 9).

In Amazonia, this same approach has also been used for the analyses of anomalies in vegetation indices from MODIS (SALESKA *et al*., 2007, ANDERSON *et al*., 2010, ATKINSON *et al*., 2011, SAMANTA *et al*., 2011) and other multi-temporal satellite data, such as SeaWinds backscattering microwave data (FROLKING *et al*. 2011, SAATCHI *et al*., 2013), and MODIS Land surface temperature (TOOMEY *et al*., 2011) as well as MODIS and AVHRR thermal anomalies (ARAGÃO *et al*., 2007). All these studies were interested in detecting the impact of droughts on forest canopy and fire incidence.

As an example, Saatchi *et al*. (2013) used data from the Ku band (13.8 GHz, ~2.2 cm) scatterometer SeaWinds onboard of the QuickSCAT platform to detect the impact and long-term recovery of Amazonian vegetation to the 2005 drought. QuickSCAT satellite is equipped with the SeaWinds active microwave sensor that operates in a Ku band frequency,

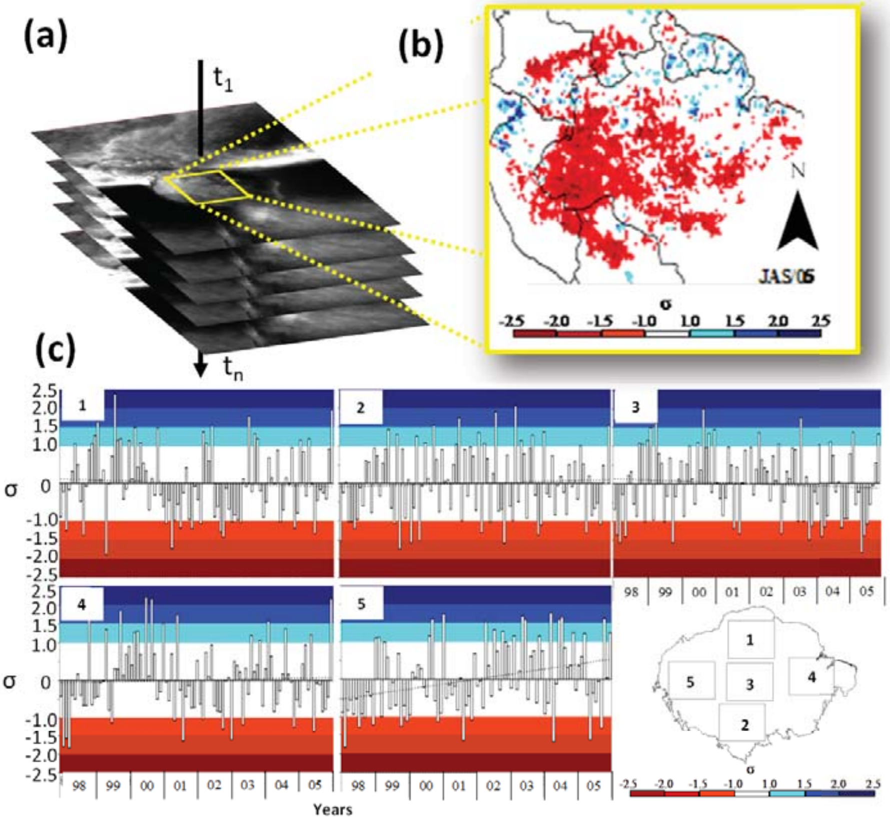

Fig. 9 - (a) Integration of monthly surfaces of rainfall derived from TRMM data for the generation of (b) pixel-by-pixel anomalies for a three-month period (July-August-September - JAS) of 2005. (c) Temporal changes in the magnitude of anomalies for five Amazonian regions, displayed in the map at the bottom right of the panel. Anomalies are measured in units of standard deviation.

with a native spatial resolution of ~25 km (FROLKING *et al*. 2011). Because of the incidence angle (~50º), the pulse emitted does not penetrate more than 5 meters into the canopy (SAATCHI *et al*., 2013). This characteristic makes this sensor an excellent alternative for detecting changes in canopy properties of forests, such as canopy water content (FROLKING *et al*., 2011) and canopy structure.

Saatchi *et al*. (2013) demonstrated that Amazonian forests experienced a decline in backscatter in an area of 2.1 million km^2 during the 2005 dry season. The region with more intense anomalies was in the southwest of Amazonia, corroborating with previous studies (ARAGÃO *et al*., 2007, ARAGÃO *et al*., 2008, FROLKING *et al*., 2011). Interesting, when comparing a region not affected by drought (Figure 10a) with one intensively affected (Figure 10b), it is clear that QuickSCAT data detects the impact of drought on forest canopy. Moreover, these data also show a slow recovery of the forest canopy after the drought (Figure 10b), which can have major implications for the dynamics of C stocks in Amazonia if drought events becomes more frequent and intense in

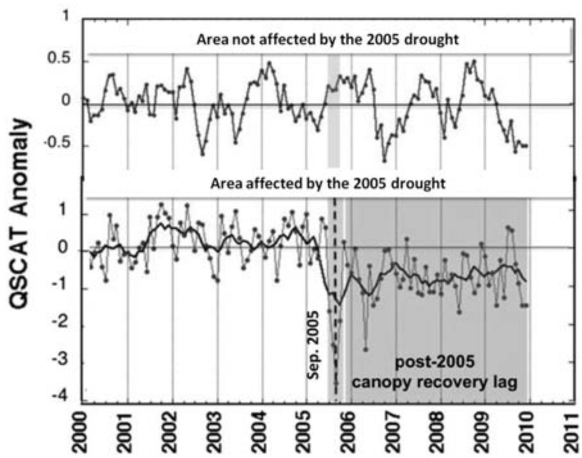

Fig. 10 - Temporal changes in anomalies derived from SeaWinds Ku band active microwave sensor from (a) a region not affect by drought and (b) the epicentre of the 2005 Amazonian drought. Note the anomalous decline in backscatter during the 2005 dry season follow by the slow recovery of the signal. Source: Saatchi *et al.* (2013).

this decade.

5. CONCLUSIONS

This review shows that over large geographical areas, as the case of Amazonia, remote sensing is perhaps the most important tool to assist the quantification of forest structure, to evaluate how vegetation changes seasonally, and to assess how the region is impacted by climate changes and how these changes affect, in turn, vegetation.

The accurate mapping of tropical forest structure, aboveground biomass and carbon stocks from regional to continental scales is nowadays a requirement for supporting climate change mitigation policies that can be achieved by using current remote sensing technologies available (especially from airborne and satellite radar sensors, and from LIDAR). However, it is crucial to keep in mind that these techniques must be supported by field-based forest surveys. The Amazon covers a vast territory with complex landscape and several anthropogenic processes operating at multiple spatial and temporal scales, with well-defined causes and effects. Therefore, in order to use this technique to support policy makers at governmental and institutional levels, there is a need to systematize procedures for mapping and inventorying forests, integrating multi-sensor data. This systematic analysis would provide maps of forest dynamics and disturbances for the entire Amazon, with a standardized method and accuracy necessary for territorial planning and biodiversity conservation.

This review also highlighted the important contribution of MODIS since 2000 for land surface phenology studies over tropical forests. The MODIS VIs product (NDVI and EVI) has been the most commonly used approach for this purpose. However, even using 16-day compositing images, cloudy data does not generally allow a reliable analysis of the VIs in the rainy season. Uncertainties in data analysis have also precluded the extensive use of the MODIS Global Vegetation Phenology Product, which is less reliable for tropical evergreen forests. Because of the uncertainties associated with atmospheric correction and view-illumination geometry, much of the phenologic studies on the Amazonian tropical forests have tried to understand the unexpected increase of MODIS EVI along the dry season and, especially, in response to severe droughts (inter-annual variations). These controversial findings, when compared to field reports of decreasing plant productivity, indicated that validation of detectable MODIS satellite phenologic patterns, using surface observations and other better spatial and spectral resolution sensors, is still necessary. For example, the combined use of MODIS/Terra and Hyperion/EO-1 has contributed to improve the understanding of the phenologic variability in the Amazonian tropical forest. When combined to LiDAR, hyperspectral sensors can be used to relate phenological variation to micro-topography and to vegetation structure. Finally, land surface phenology studies can benefit from the transition from low to high signal-to-noise (SNR) orbital imaging spectrometers, and especially from sampling (e.g., Hyperion/EO-1 with 7.7 km of swath width) to global coverage hyperspectral missions. This is the case of the proposed NASA HyspIRI mission, to be launched in near future, with 150 km of swath width, more than 200 bands, 60 m of spatial resolution and with 19 days revisit time.

Remote sensing has also played an important role in quantifying the impacts of natural and human-driven disturbances or changes that can directly impact the Amazon biome carbon balance. Deforestation, selective logging and forest fires are the main human-driven disturbances occurring in Amazonia. The use of data from Landsat sensors and MODIS has improved our understanding on the extent, spatial configuration and recurrence time of these events. However, there is an urgent need to improve not only the long-term quantification of both extent of impacts of selective logging and fire, but also the evaluation of the recovery time of these areas.

Orbital microwave technology enhanced our capacity to measure spatially explicit changes of rainfall patterns in Amazonia and how this variable does varies temporally. Moreover, this same technology allowed the identification of slow recovery of the forest canopy after the drought. One key aspect that must be better understood is the biophysical meaning of the information. Therefore, long-term systematic field surveys are urgently required to resolve this gap in our knowledge.

Changes in forest structure and functioning can have major implications for the dynamics of C stocks in Amazonia if drought events become more frequent and intense in this decade. Therefore, remote sensing is likely to be at the front of this scientific field for many years to come as a scientific tool to support the conservation and management of natural resources in Amazonia. These are, at present, the most pressing demands of society, government, and non-governmental organizations, which see Amazonia as an important component of the Earth system that can help in alleviating or mitigating the impacts of climate and environmental changes.

ACKNOWLEDGMENTS

J.R. Santos and L.S. Galvão acknowledge the support of the São Paulo Research Foundation (FAPESP) (Grants 2008/11499-8 and 2013/03908-3) and CNPq (*Conselho Nacional de Desenvolvimento Científico e Tecnológico*). L.E.O.C. Aragão acknowledges the support of the UK Natural Environment Research Council (NERC) grants (NE/F015356/2 and NE/l018123/1) and the CNPq and CAPES for the Science without Borders Program's Fellowship.

REFERENCES

ADAMS, J. B.; SABOL, D. E.; KAPOS, V.; FILHO, R. A.; ROBERTS, D. A.; SMITH, M. O.;GILLESPIE, A. R. Classification of multispectral images based on fractions of endmembers: Application to land-cover change in the Brazilian Amazon. **Remote Sensing of Environment**, v. 52, p. 137 – 154, 1995.

AGUIAR, A.P.D.; OMETTO, J.P.; NOBRE, C.; LAPOLA, D.M.; ALMEIDA, C.; VIEIRA, I.C.; SOARES, J.V.; ALVALA, R.; SAATCHI, S.; VALERIANO, D.; CASTILLA-RUBIO, J.C. Modeling the spatial and temporal heterogeneity of deforestation-driven carbon emissions: the INPE-EM framework applied to the Brazilian Amazon. **Global Change Biology**, v. 18, p.3346 - 3366, 2012.

AHL, D. E.; GOWER, S. T.; BURROWS, S. N.; SHABANOV, N. V.; MYNENI, R. B.; KNYAZIKHIN, Y. Monitoring spring canopy phenology of a deciduous broadleaf forest using MODIS. **Remote Sensing of Environment,** v. 104, p. 88−95, 2006.

ALENCAR, A.; ASNER, G. P.; KNAPP, D.; ZARIN, D. Temporal variability of forest fires in eastern Amazonia. **Ecological Applications**, v. 21(7), p. 2397-2412, 2011.

ANDERSON, L. O. Biome-Scale Forest Properties in Amazonia Based on Field and Satellite Observations. **Remote Sensing,** v. 4, p. 1245-1271, 2012.

ANDERSON, L. O.; ARAGÃO, L. E. O.; LIMA, A. D.; SHIMABUKURO, Y. E. Burn scar detection based on linear mixture model and vegetation indices using multitemporal data from MODIS/TERRA sensor in Mato Grosso State, Brazilian Amazon. **Acta Amazonica**, v. 35(4), p. 445-456, 2005.

ANDERSON, L. O.; MALHI, Y.; ARAGÃO, L. E. O. C.; LADLE, R.; ARAI, E.; BARBIER, N.; PHILLIPS, O. Remote sensing detection of droughts in Amazonian forest canopies. **The New Phytologist,** v. 187, p. 733–750, 2010.

ANDERSON, L.O.; SHIMABUKURO, Y.E. ; DEFRIES, R.S.; MORTON, D. Assessment of deforestation in near real time over the Brazilian Amazon using multitemporal fraction images derived from Terra MODIS. **IEEE Geoscience and Remote Sensing Letters**, v. 2(3), p. 315 – 318, 2005.

ARAGÃO, L. E. O. C.; MALHI, Y.; BARBIER, N.; LIMA, A.; SHIMABUKURO, Y.; ANDERSON, L.; SAATCHI, S. Interactions between rainfall, deforestation and fires during recent years in the Brazilian Amazonia. **Philosophical Transactions of the Royal Society B-Biological Sciences**, v. 363 (1498), p. 1779-1785, 2008.

ARAGÃO, L. E. O. C.; MALHI, Y.; ROMAN-CUESTA, R. M.; SAATCHI, S.; ANDERSON, L. O.; SHIMABUKURO, Y. E. Spatial patterns and fire response of recent Amazonian droughts. **Geophysical Research Letters,** v. 34, L07701, 2007.

ASNER, G. P.; KELLER, M.; PEREIRA, JR, R.; ZWEEDE, J. C.; SILVA, J. N. Canopy damage and recovery after selective logging in Amazonia: field and satellite studies. **Ecological**

Applications, v. 14(sp4), p. 280-298, 2004.

ASNER, G. P.; ALENCAR, A. Drought impacts on the Amazon forest: The remote sensing perspective. **The New Phytologist,** v. 187, n. 3, p. 569–578, 2010.

ASNER, G. P.; KNAPP, D. E.; BOARDMAN, J.; GREEN, R. O.; KENNEDY-BOWDOIN, T.; EASTWOOD, M.; MARTIN, R. E.; ANDERSON, C.; FIELD, C. B. Carnegie Airborne Observatory-2: Increasing science data dimensionality via high-fidelity multi-sensor fusion. **Remote Sensing of Environment,** v. 124, p. 454-465, 2012.

ATKINSON, P. M.; DASH, J.; JEGANATHAN, C. Amazon vegetation greenness as measured by satellite sensors over the last decade. **Geophysical Research Letters**, v. 38(19), L19105, 2011.

BRADLEY, A. V.; GERARD, F. F.; BARBIER, N.; WEEDON, G. P.; ANDERSON, L. O.; HUNTINGFORD, C.; ARAGÃO, L. E. O. C.; ZELAZOWSKI, P.; ARAI, E. Relationships between phenology, radiation and precipitation in the Amazon region. **Global Change Biology,** v. 17, p. 2245–2260, 2011.

BRANDO, P. M.; GOETZ, S. J.; BACCINI, A.; NEPSTAD, D. C.; BECK, P. S. A.; CHRISTMAN, M. C. Seasonal and interannual variability of climate and vegetation indices across the Amazon. **Proceedings of the National Academy of Sciences (PNAS),** v. 107, n. 33, p. 14685–14690, 2010.

BREUNIG, F. M.; GALVÃO, L. S.; FORMAGGIO, A. R.; EPIPHANIO, J. C. N. Directional effects on NDVI and LAI retrievals from MODIS: A case study in Brazil with soybean. **International Journal of Applied Earth Observation and Geoinformation,** v. 13, n. 1, p. 34–42, 2011.

CHÁIDEZ, J.J.N. Allometric equations and expansion factors for tropical try forest trees of eastern Sinaloa, Mexico. **Tropical and Subtropical Agroecosystems**, v.10, n.1, p.45 - 52, 2009.

CHAZDON, R. L.; REDONDO BRENES, A.; VILCHEZ ALVARADO, B. Effects of climate and stand age on annual tree dynamics in tropical second-growth rain forests. **Ecology**, v. 86, p. 1808 - 1815, 2005.

CLARK, D. B., CLARK, D. A. Landscape-scale variation in forest structure and biomass in a tropical rain forest. **Forest Ecology and Management**, v.137, p.185 - 198, 2000.

CLARK, D. B.; CLARK, D. A.; RICH, P. M; WEISS, S.; OBERBAUER, S. F. Landscape scale evaluation of understory light and canopy structure: Methods and application to a neotropical lowland rain forest. **Canadian Journal of Forest Research**, v. 26, n.5, p. 747 - 757, 1996.

CLARK, D. Sources or sinks? The responses of tropical forests to current and future climate and atmospheric composition. **Philosophical Transactions of the Royal Society B**, v.359, n.1443, p. 47- 91, 2004.

CLOUDE, S. R.; POTTIER, E. An entropy based classification scheme for land application of polarimetric SAR. **IEEE Transactions on Geoscience and Remote Sensing**, v.35, n.1, p.68-78, 1997.

CLOUDE, S.R., PAPATHANASSIOU, K.P. Forest vertical structure estimation using coherence tomography. In: IEEE International Geoscience and Remote Sensing Symposium - IGARSS, Boston, USA, 7–11 July, 2008. **IEEE Proceedings**, p. 275–278.

CLOUDE, S.R.; BROLLY, M.; WOODHOUSE, I.H. A study of forest vertical structure estimation using coherence tomography coupled to a macro-ecological scattering model. In: IEEE International Geoscience and Remote Sensing Symposium - IGARSS, Cape Town, South Africa, 12-17 July, 2009. **IEEE Proceedings**, v.44, p. 717 - 720. DOI: 10.1109/IGARSS.2009.5417477

COCHRANE, M. A. Linear mixture model classification of burned forests in the eastern Amazon. **International Journal of Remote Sensing**, v. 19(17), p. 3433-3440, 1998.

COCHRANE, M. A.; LAURANCE, W. F. Synergisms among Fire, Land Use, and Climate Change in the Amazon. **AMBIO: A Journal of the Human Environment**, v. 37 (7), p. 522-527, 2008.

COX, P.M.; BETTS, R.A.; COLLINS, M.,

HARRIS, P.P.; HUNTINGFORD, C.; JONES, C.D. Amazonian forest dieback under climate-carbon cycle projections for the 21st century. **Theoretical and Applied Climatology**, v.78, n.1-3, p.137-156. 2004.

DEFRIES, R.S. *et al*. Carbon emissions from tropical deforestation and regrowth based on satellite observations for the 1980s and 90s. **Proceedings of the National Academy of Sciences**, v. 99, n. 22, p. 14256-14261, 2002.

DINH, H.T.M.; LE TOAN, T.; ROCCA, F.; TEBALDINI, S.; d'ALESSANDRO, M.M.; VILLARD, L. Relating P-band synthetic aperture radar tomography to tropical forest biomass. **IEEE Transactions on Geoscience and Remote Sensing**, 13p. 2013. DOI: 10.1109/TGRS.2013.2246170.

EVA, H. D.; HUBER, O. A Proposal for defining the geographical boundaries of Amazonia. European Commission - Luxembourg: **Office for Official Publications of the European Communities** 2005. ISBN 92-79-00012-8, 2005.

FREEMAN, A.; S.L.DURDEN. *A three-component scattering model for polarimetric SAR data*. **IEEE Transactions on Geoscience and Remote Sensing**, v. 36, n.3, p. 963 - 973, 1998.

FROLKING, S.; MILLIMANA, T.; PALACEA, M.; WISSERA, D.; LAMMERSA, R.; FAHNESTOCKA, M. Tropical forest backscatter anomaly evident in SeaWinds scatterometer morning overpass data during 2005 drought in Amazonia. **Remote Sensing of Environment,** v. 115, n. 3, p. 897–907, 2011.

GALVÃO, L. S.; BREUNIG, F. M.; SANTOS, J. R.; MOURA, Y. M. View-illumination effects on hyperspectral vegetation indices in the Amazonian tropical forest. **International Journal of Applied Earth Observation and Geoinformation,** v. 21, p. 291–300, 2013.

GALVÃO, L. S.; SANTOS, J. R.; ROBERTS, D. A.; BREUNIG, F. M.; TOOMEY, M.; MOURA, Y. M. On intra-annual EVI variability in the dry season of tropical forest: A case study with MODIS and hyperspectral data. **Remote Sensing of Environment,** v. 115, n. 9, p. 2350–2359, 2011.

GANGULY, S.; FRIEDL, M. A.; TAN, B.; ZHANG, X.; VERMA, M. Land surface phenology from MODIS: Characterization of the Collection 5 global land cover dynamics product. **Remote Sensing of Environment,** v. 114, p. 1805–1816, 2010.

GAO, F.; MORISETTE, J. T.; WOLFE, R.E.; EDERER, G.; PEDELTY, J.; MASUOKA, E.; MYNENI, R.; TAN, B.; NIGHTINGALE, J. An algorithm to produce temporally and spatially continuous MODIS-LAI time series. **IEEE Transactions on Geoscience and Remote Sensing Letters,** v. 5, p. 60–64, 2008.

GIBBS, H.K., BROWN, S.; NIELES, J.O.; FOLEY, J.A. Monotoring and estimatinf tropical forest carbon stocks: making REDD a reality. **Environmental Research Letters**, v. 2, n. 045023, 13p., 2007.

GONÇALVES, F. G.; SANTOS, J. R.; TREUHAFT, R.N. Stem volume of tropical forests from polarimetric radar. **International Journal of Remote Sensing**, v. 32, n. 2, p.503 -522, 2011.

HEIMANN, M.; ESSER, G.; HAXELTINE, A.; KADUK, J.;KICKLIGHTER, D. W.; KNORR, W.; KOHLMAIER, G. H.; MCGUIRE, A. D.; MELILLO, J.; MOORE, B.; OTTO, R. D.; PRENTICE, I. C.; SAUF, W.; SCHLOSS, A.; SITCH, S.; WITTENBERG, U.; WURTH, G. Evaluation of terrestrial Carbon Cycle models through simulations of the seasonal cycle of atmospheric CO_2: First results of a model intercomparison study. **Global Biogeochemical Cycles,** v. 12, n. 1, p. 1-24, 1998.

HENDERSEN, F.M.; LEWIS, A.J. Radar fundamentals: The geoscience perspective. In: Ryerson, R.A. (ed.), Manual of Remote Sensing: Principles and Applications of Imaging Radar. 3. ed. New York, John Wiley & Sons, Inc., v.2, cap.3, p.131-181, 1998.

HMIMINA, G.; DUFRENE, E.; PONTAILLER, J. Y.; DELPIERRE, N.; AUBINET, M.; CAQUET, B.; GRANDCOURT, A.; BURBAN, B.; FLECHARD, C.; GRANIER, A.; GROSS, P.; HEINESCH, B.; LONGDOZ, B.; MOUREAUX, C.; OURCIVAL, J. M.; RAMBAL, S.; SAINT ANDRE, L.; SOUDANI, K. Evaluation of the potential of MODIS satellite data to predict vegetation phenology in different biomes: An investigation using ground-based NDVI measurements. **Remote Sensing of Environment,** v. 132, p. 145-158, 2013.

HOEKMAN, D. H.; QUIÑONES, M. J. Land cover type and biomass classification using AirSAR data for evaluation of monitoring scenarios in the Colombian Amazon. **IEEE Transactions Geoscience and Remote Sensing**, v.38, n.2, p.685 - 696, 2000.

HOU, Z.; XU, Q., TOKOLA, T. Use of ALS, airborne CIR and ALOS ABVIR-2 data for estimating tropical Forest attributes in Lao PDR. **ISPRS Journal of Photogrammetry and Remote Sensing**. v. 66, p. 776 - 786, 2011.

HOUGHTON, R. A.; SKOLE, D. L.; NOBRE, C. A.; HACKLER, J. L.; LAWRENCE, K. T.; CHOMENTOWSKI, W. H. Annual fluxes of carbon from deforestation and regrowth in the Brazilian Amazon. **Nature**, v. 403, p. 301-304., 2000.

HUETE, A. R.; DIDAN, K.; SHIMABUKURO, Y. E.; RATANA, P.; SALESKA, S. R.; HUTYRA, L. R.; YANG, W.; NEMANI, R. R.; MYNENI, R. Amazon rainforests green-up with sunlight in dry season. **Geophysical Research Letters,** v. 33, L06405, 2006.

HUETE, A. R.; KIM, Y.; RATANA, P.; DIDAN, K.; SHIMABUKURO, Y. E.; MIURA, T. Assessment of phenologic variability in Amazon tropical rainforests using hyperspectral Hyperion and MODIS satellite data. In: Kalacska, M.; Sanchez-Azofeifa, G.A. (Eds.). **Hyperspectral Remote Sensing of Tropical and Sub-tropical Forests**. CRC Press, Taylor and Francis Group, Boca Raton, FL, pp. 233–259 (Chapter 11), 2008.

HUETE, A.; DIDAN, K.; MIURA, T.; RODRIGUEZ, E. P.; GAO, X.; FERREIRA, L. G. Overview of the radiometric and biophysical performance of the MODIS vegetation indices. **Remote Sensing of Environment,** v. 83, p. 195−213, 2002.

HUTYRA, L. R.; MUNGER, J. W.; NOBRE, C.A., SALESKA, S. R.; VIEIRA, S. A.; WOFSY, S. C. Climatic variability and vegetation vulnerability in Amazonia. **Geophysical Research Letters**, 2005, 32, L24712, doi:10.1029/2005GL024981.

IPCC Fourth Assessment Report: Climate Change 2007 (AR4). Model output described in the 2007 IPCC Fourth Assessment Report (SRES scenarios), multi-year means, available at http://www.ipcc-data.org/ar4/gcm_data.html

KOCH, B. Status and future of laser scanning, synthetic aperture radar and hyperspectral remote sensing data for forest biomass assessment. **ISPRS Journal of Photogrammetry and Remote Sensing**. v. 65, p.581-590., 2010.

KUGLER, F.; PAPATHANASSIOU, K.P.; HAJNSEK, I. Forest height estimation over tropical forest by means of polarimetric SAR interferometry. In: Seminário de Atualização em Sensoriamento Remoto e Sistemas de Informações Geográficas Aplicados à Engenharia Florestal, 7., Curitiba, Paraná, 17-19 out., 2006. **Anais**. p.504-512. [CDROM].

LI, W. H., FU, R., DICKINSON, R. E. Rainfall and its seasonality over the Amazon in the 21st century as assessed by the coupled models for the IPCC AR4. **Journal of Geophysical Research-Atmospheres**, 2006, 111, D02111, doi:10.1029/2005JD006355.

LIANG, L.; SCHWARTZ, M. D.; FEI, S. Validating satellite phenology through intensive ground observation and landscape scaling in a mixed seasonal forest. **Remote Sensing of Environment,** v. 115, p. 143-157, 2011.

LIMA, A.; SILVA, T. S. F.; FEITAS, R. M. D.; ADAMI, M.; FORMAGGIO, A. R.; SHIMABUKURO, Y. E. Land use and land cover changes determine the spatial relationship between fire and deforestation in the Brazilian Amazon. **Applied Geography**, v. 34, p. 239-246, 2012.

LOMBARDINI, F.; CAL, F.; VIVIANI, F. Forest "dynamic" tomography: height-varying temporal coherence separation. Tyrrhenian Workshop on Advances in Radar and Remote Sensing (TyWRRS). Naples, 12-14 Sept., 2012. **Proceedings**. p.94-99.

LU, D., MORAN, E., BATISTELLA, M. Linear mixture model applied to Amazonian vegetation classification. **Remote Sensing of Environment**, v. 87, p. 456 – 469, 2003.

MALHI, Y., ROBERTS, J.T., BETTS, R.A.,

KILLEEN, T.J., LI, W., NOBRE, C.A. Climate change, deforestation and the fate of the Amazon. **Science**, v. 319(5860), p. 169-172, 2008.

MALHI, Y.; NOBRE, A. D., GRACE, J.; KRUIJT B.; PEREIRA M. G. P.; CULF A.; SCOTT, S. Carbon dioxide transfer over a Central Amazonian rain forest. **Journal of Geophysical Research-Atmospheres**, v.103, p. 31593-31612, 1998.

MARENGO, J. A.; TOMASELLA, J.; ALVES, L. M.; SOARES, W. R.; RODRIGUEZ, D. A. The drought of 2010 in the context of historical droughts in the Amazon region, **Geophysical Research Letters**, 2011, 38, L12703, doi:10.1029/2011GL047436.

MATRICARDI, E. A.; SKOLE, D. L.; PEDLOWSKI, M. A.; CHOMENTOWSKI, W.; FERNANDES, L. C. Assessment of tropical forest degradation by selective logging and fire using Landsat imagery. **Remote Sensing of Environment**, v. 114(5), p. 1117-1129, 2010.

MCT – Ministério da Ciência e Tecnologia do Brasil. Segunda Comunicação Nacional do Brasil à Convenção- Quadro das Nações Unidas sobre Mudança Climática. Brasília/ DF. 520 p, 2010.

MELAAS, E. K.; FRIEDL, M. A.; ZHU, Z. Detecting interannual variation in deciduous broadleaf forest phenology using Landsat TM/ ETM+ data. **Remote Sensing of Environment,** v. 132, p. 176-185, 2013.

MORISETTE, J. T.; PRIVETTE, J. L.; JUSTICE, C. O. A framework for the validation of MODIS land products. **Remote Sensing of Environment,** v. 83, p. 77−96, 2002.

MORTON, D. C., DEFRIES, R. S., NAGOL, J., SOUZA JR, C. M., KASISCHKE, E. S., HURTT, G. C., DUBAYAH, R. Mapping canopy damage from understory fires in Amazon forests using annual time series of Landsat and MODIS data. **Remote Sensing of Environment**, v. 115(7), p. 1706-1720, 2011.

MORTON, D. C.; LE PAGE, Y.; DEFRIES, R.; COLLATZ, G. J.; HURTT, G. C. Understorey fire frequency and the fate of burned forests in southern Amazonia. **Philosophical Transactions of the Royal Society B: Biological Sciences**, v. 368(1619), p.1-8, 2013.

MOURA, Y.M.; GALVÃO, L. S.; SANTOS, J. R.; ROBERTS, D. A.; BREUNIG, F. M. Use of MISR/Terra data to study intra- and inter-annual EVI variations in the dry season of tropical forest. **Remote Sensing of Environment,** v. 127, p. 260-270, 2012.

NARVAES, I.S. Avaliação de dados SAR polarimétricos para estimativa de biomassa em diferentes fitofisionomias de florestas tropicais. Tese de Doutorado: INPE, 2010. 168p sid.inpe. br/mtc-m19@80/2010/08.09.22.43-TDI).

NEEFF, T; . DUTRA, L.V.; SANTOS, J.R.; FREITAS, C.C.; ARAUJO, L.S. Tropical forest stand table modelling from SAR data. **Forest Ecology and Management**, v.186, p.159 - 170, 2003.

NICOTRA, A. B.; CHAZDON, R. L.; IRIARTE, S. V. B. Spatial heterogeneity of light and woody seedling regeneration in tropical wet forests. **Ecology,** v. 80, p. 1908 - 1926. 1999.

PAN, Y.; BIRDSEY, R. A.; FANG, J.; HOUGHTON, R.; KAUPPI, P. E.; KURZ, W. A.; HAYES, D. A large and persistent carbon sink in the world’s forests. **Science**, v. 333 (6045), p. 988-993, 2011.

PHILLIPS, O. L.; ARAGÃO, L. E.; LEWIS, S. L.; FISHER, J. B.; LLOYD, J.; LÓPEZ-GONZÁLEZ, G.; ANDRADE, A. Drought sensitivity of the Amazon rainforest. **Science**, v. 323(5919), p. 1344-1347, 2009.

POPE, K.O.; REY-BENAYAS, J.M.; PARIS, J.F. Radar remote sensing of forest and wetland ecosystems in Central American Tropics. **Remote Sensing of Environment**, v.2, n.48, p.205 - 219, 1994.

RICHARDS, P. W. **The tropical rain forest: an ecological study**. (2nd ed.). Cambridge: Cambridge University Press, 1996. 600p. ISBN:9780521421942.

RICHARDSON, A. D.; JENKINS, J.; BRASWELL, B.; HOLLINGER, D.; OLLINGER, S.; SMITH, M. L. Use of digital webcam images to track spring green-up in a deciduous broadleaf forest. **Oecologia,** v. 152, p. 323–334, 2007.

ROBERTS, D. A.; ROTH, K. L.; PERROY, R. L. Hyperspectral vegetation indices. In: Thenkabail, P. S.; Lyon, J. G.; Huete, A. (Eds.), **Hyperspectral Remote Sensing of Vegetation**. CRC Press, Taylor and Francis Group, Boca Raton, FL, pp. 309–327, 2012. (Chapter 14).

SAATCHI, S.; ASEFI-NAJAFABADY, S.; MALHI, Y.; ARAGÃO, L. E.; ANDERSON, L. O.; MYNENI, R. B.; NEMANI, R. Persistent effects of a severe drought on Amazonian forest canopy. **Proceedings of the National Academy of Sciences**, v. 110(2), p. 565-570, 2013.

SAATCHI, S.; MARLIER, M.; CHAZDON, R.L.; CLARK, D.B.; RUSSEL, A.E. Impact of spatial variability of tropical forest structure on radar estimation of aboveground biomass. **Remote Sensing of Environment,** v.115, p.2836 - 2849, 2011.

SAATCHI, S.S. Synergism of optical and radar data for forest structure and biomass. **Ambiência,** Guarupava (PR), v.6, Ed. Especial, p. 151-166, 2010.

SAATCHI, S.S.; HOUGHTON, R.A.; ALVALÁ, R.C.S.; SOARES, J.V.; YU, Y. Distribution of aboveground live biomass in the Amazon basin. **Global Change Biology**, v.13, p. 816 - 837, 2007.

SALESKA, S. R.; DIDAN, K.; HUETE, A. R.; ROCHA, H. R. Amazon forests green-up during 2005 drought. **Science**, v. 318(5850), p. 612-612, 2007.

SAMANTA, A.; GANGULY, S.; MYNENI, R. B. MODIS Enhanced Vegetation Index data do not show greening of Amazon forests during the 2005 drought. **New Phytologist**, v. 189(1), p. 11-15, 2011.

SAMANTA, A.; GANGULY, S.; HASHIMOTO, H.; DEVADIGA, S.; VERMOTE, E.; KNYAZIKHIN, Y.; MYNENI, R. B. Amazon forests did not green-up during the 2005 drought. **Geophysical Research Letters**, v. 37(5), (2010). DOI: 10.1029/2009GL042154.

SANTOS, J.R.; FREITAS, C.C.; ARAUJO, L.S.; DUTRA, L.V.; MURA, J.C.; GAMA, F.F.; SOLER, L.S.; SANT'ANNA, S.J.S. Airborne P-band SAR applied to the aboveground biomass studies in the Brazilian tropical rainforest. **Remote Sensing of Environment**, v.87, n.4, p.482 - 493, 2003.

SANTOS, J.R.; NARVAES, I.S.; GRAÇA, P.M.L.A.; GONÇALVES, F.G. Analysis of ALOS/PALSAR polarimetric signatures and scattering mechanisms of forest types in Tapajós region, Brazil. In: ALOS PI 2008 Symposium. Rhodes, Greece, 3-7 nov., 2008. **Proceedings**. [CDROM]. [ESA SP 664].

SANTOS, J.R.; NARVAES, I.S.; P.M.L.A.G.; GONÇALVES, F.G. **Polarimetric responses and scattering mechanisms of tropical forests in the Brazilian Amazon**. In: Advances in Geoscience and Remote Sensing. Ed. Gary Jedlovec, In-Tech, Croatia, p.183 - 206, 2009.

SCHAAF, C. B.; GAO, F.; STRAHLER, A. H.; LUCHT,W.; LI, X. W.; TSANG, T.; STRUGNELL, N. C.; ZHANG, X. Y.; JIN, Y. F.; MULLER, J. P.; LEWIS, P.; BARNSLEY, M.; HOBSON, P.; DISNEY, M.; ROBERTS, G.; DUNDERDALE, M.; DOLL, C.; D'ENTREMONT, R. P.; HU, B. X.; LIANG, S. L.; PRIVETTE, J. L.; ROY, D. First operational BRDF, albedo nadir reflectance products from MODIS. **Remote Sensing of Environment,** v. 83, n. 1-2, p. 135–148, 2002.

SCHAEPMAN, M. E.; USTIN, S. L.; PLAZA, A. J.; PAINTER, T. H.; VERRELST, J.; LIANG, S. L. Earth system science related imaging spectroscopy: An assessment. **Remote Sensing of Environment,** v. 113, p. S123-S137, 2009.

SHIMABUKURO, Y. E.; DUARTE, V.; ARAI, E.; FREITAS, R. M.; LIMA, A.; VALERIANO, D. M.; MALDONADO, M. L. R. Fraction images derived from Terra Modis data for mapping burnt areas in Brazilian Amazonia. **International Journal of Remote Sensing**, v. 30(6), p. 1537-1546, 2009.

SHIMABUKURO, Y.E.; BATISTA, G.T.; MELLO, E.M.K.; MOREIRA, J.C.; DUARTE, V. Using shade fraction image segmentation to evaluate deforestation in Landsat Thematic Mapper images of the Amazon region**.** **International Journal of Remote Sensing**, v. 19(3), p. 535-541, 1998.

SKOLE D.; TUCKER C. Tropical deforestation and habitat fragmentation in the Amazon: satellite data from 1978 to 1988**.** **Science**, v.

260(5116), p. 1905-1910, 1993.

SOUDANI, K.; HMIMINA, G.; DELPIERRE, N.; PONTAILLER, J. Y.; AUBINET, M.; BONAL, D.; CAQUET, B.; GRANDCOURT, A.; BURBAN, B.; FLECHARD, C.; GUYON, D.; GRANIER, A.; GROSS, P.; HEINESH, B.; LONGDOZ, B.; LOUSTAU, D.; MOUREAUX, C.; OURCIVAL, J. M.; RAMBAL, S.; SAINT ANDRÉ, L.; DUFRÊNE, E. Ground-based Network of NDVI measurements for tracking temporal dynamics of canopy structure and vegetation phenology in different biomes. **Remote Sensing of Environment,** v. 123, p. 234-245, 2012.

SPRACKLEN, D. V.; ARNOLD, S. R.; TAYLOR, C. M. Observations of increased tropical rainfall preceded by air passage over forests. **Nature**, v. 489, p. 282–285 2012.

TAN, B.; MORISETTE, J. T.; WOLFE, R. E.; GAO, F.; EDERER, G. A.; NIGHTINGALE, J.; PEDELTY, J. A. An enhanced TIMESAT algorithm for estimating vegetation phenology metrics from MODIS data. **IEEE Journal of Selected Topics in Applied Earth Observations and Remote Sensing,** v. 4, n. 2, p. 361-371, 2011

TOOMEY, M.; ROBERTS, D. A.; STILL, C.; GOULDEN, M. L.; MCFADDEN, J. P. Remotely sensed heat anomalies linked with Amazonian forest biomass declines. **Geophysical Research Letters**, v.38(19), 2011. DOI: 10.1029/2011GL049041.

TOUZI, R. Target scattering decomposition in terms of roll-invariant target parameters. **IEEE Transactions on Geoscience and Remote Sensing**, v. 45, p. 73-84, 2007.

TOUZI, R.; DESCHAMPS, A.; ROTHER, G. Phase of target scattering for wetland characterization using polarimetric C-band SAR. **IEEE Transactions on Geoscience and Remote Sensing**, v. 47, n. 9, p. 3241-3261, 2009.

TREUHAFT, R. N.; CHAPMAN, B. D.; SANTOS, J. R.; GONÇALVES, F. G.; DUTRA, L. V.; GRAÇA, P. M. L. A.; DRAKE, J. B. Vegetation profiles in tropical forests from multibaseline interferometric synthetic aperture radar, field, and lidar measurements. **Journal of Geophysical Research**. v., 114, p. D23110, 2009. DOI:10.1029/2008JD011674.

TREUHAFT, R.N.; GONÇALVES, F.G.; DRAKE, J.; CHAPMAN, B.; SANTOS, J.R.; DUTRA, L.V.; GRAÇA, P. M.L.A.; PURCELL, G.H., 2010. Biomass estimation in a tropical wet forest using Fourier transforms of profiles from Lidar or Interferometric SAR. **Geophysical Research Letters**, v.37, p. L23403, 2010.

VAN ZYL, J.J.; ZEBKER, H.A.; ELACHI, C. Imaging radar polarimetric signatures: theory and observation. **Radio Science**, v.22, n.4, p.529 - 543, 1987.

VERBESSELT, J.; HYNDMAN, R.; ZEILEIS, A.; CULVENOR, D. Phenological change detection while accounting for abrupt and gradual trends in satellite image time-series. **Remote Sensing of Environment,** v. 114, p. 2970–2980, 2010.

WOODHOUSE, I. H. Introduction to microwave remote sensing, Boca Raton: Taylor & Francis Group CRC Press, 2006. 370 p.

XU, L.; SAMANTA, A.; COSTA, M. H.; GANGULY, S. Widespread decline in greenness of Amazonian vegetation due to the 2010 drought. **Geophysical Research Letters,** v. 38, (article L07402), 2011.

ZENG, N.; YOON, J. H.; MARENGO, J. A.; SUBRAMANIAM, A.; NOBRE, C. A.; MARIOTTI, A.; NEELIN, J. D. Causes and impacts of the 2005 Amazon drought. **Environmental Research Letters**, 3(1), 014002, 2008.

ZHANG, X.; FRIEDL, M. A.; SCHAAF, C. B. Global vegetation phenology from Moderate Resolution Imaging Spectroradiometer (MODIS): Evaluation of global patterns and comparison with in situ measurements. **Journal of Geophysical Research,** v. 111, G0401, 2006.